# Thermodynamic Properties of Gaseous Ruthenium Species

**ARTICLE** *in* THE JOURNAL OF PHYSICAL CHEMISTRY A · APRIL 2015

Impact Factor: 2.69 · DOI: 10.1021/acs.jpca.5b01645 · Source: PubMed

THE JOURNAL OF PHYSICAL CHEMISTRY A

Article

pubs.acs.org/JPCA

# Thermodynamic Properties of Gaseous Ruthenium Species

Faoulat Miradji,[†,‡,§,∥] Sidi Souvi,[†,∥] Laurent Cantrel,[†,∥] Florent Louis,[‡,∥] and Valérie Vallet*[,§]

[†]Institut de Radioprotection et de Sûreté Nucléaire (IRSN), PSN-RES, Cadarache, St Paul Lez Durance 13115, France

[‡]PhysicoChimie des Processus de Combustion et de l'Atmosphère (PC2A), UMR 8522 CNRS/Lille1, Université Lille 1 Sciences et Technologies, Cité Scientifique, Bât C11/C5, F-59655 Villeneuve d'Ascq, Cedex, France

[§]Physique des Lasers Atomes et Molécules (PhLAM), UMR 8523 CNRS/Lille1, Université de Lille, F-59655 Villeneuve d'Ascq, Cedex 59655, France

[∥]Laboratoire de Recherche Commun IRSN-CNRS-Lille1 "Cinétique Chimique, Combustion, Réactivité" (C3R), Cadarache, Saint Paul Lez Durance 13115, France

Supporting Information

**ABSTRACT:** The review of thermodynamic data of ruthenium oxides reveals large uncertainties in some of the standard enthalpies of formation, motivating the use of high-level relativistic correlated quantum chemical methods to reduce the level of discrepancies. The reaction energies leading to the formation of ruthenium oxides RuO, $RuO_2$, $RuO_3$, and $RuO_4$ have been calculated for a series of reactions. The combination of different quantum chemical methods has been investigated [DFT, CASSCF, MRCI, CASPT2, CCSD(T)] in order to predict the geometrical parameters, the energetics including electronic correlation and spin−orbit coupling. The most suitable method for ruthenium compounds is the use of TPSSh-5%HF for geometry optimization, followed by CCSD(T) with complete basis set (CBS) extrapolations for the calculation of the total electronic energies. SO-CASSCF seems to be accurate enough to estimate spin−orbit coupling contributions to the ground-state electronic energies. This methodology yields very accurate standard enthalpies of formations of all species, which are either in excellent agreement with the most reliable experimental data or provide an improved estimate for the others. These new data will be implemented in the thermodynamical databases that are used by the ASTEC code (accident source term evaluation code) to build models of ruthenium chemistry behavior in severe nuclear accident conditions. The paper also discusses the nature of the chemical bonds both from molecular orbital and topological view points.

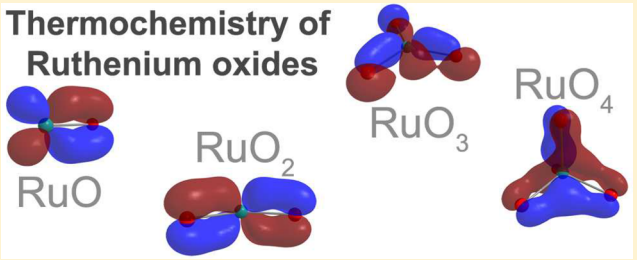


## INTRODUCTION

During a severe accident occurring in a pressurized water reactor (PWR), fission products (FPs) are released from the nuclear fuel and may reach the nuclear reactor containment building. Among the FPs, ruthenium is of particular interest due to its ability to form volatile oxide compounds in highly oxidizing conditions, and its potential high contribution to the dose in case of outside releases, in the short term, via isotope $^{103}$Ru (half-life of 39.3 days), and in the midterm, via isotope $^{106}$Ru (half-life of 372.6 days).

A literature survey[1] was carried out about ruthenium behavior in severe accident conditions based on quite old works. It was concluded that additional data are required in order to make a reliable assessment of the ruthenium outside releases in case of severe accident. Since this literature survey in 1986, many works were performed on this topic[2−12] to fill the gap in the prediction of ruthenium behavior. Ruthenium is usually considered as a low volatile fission product, with less than 5% releases, but in some conditions involving ruthenium oxides formation, as shown during the VERCORS HT2 tests[9] dealing with the fission product release from $UO_2$ fuel with a moderate burn-up [48 (GWd/tU)], in pure steam, the ruthenium released amounted to 60% of the fuel inventory and a relevant part (12%) was transported as the oxide form and not deposited in the experimental line, even at quite a low temperature (150 °C). Some modelings were performed[7,10] to predict ruthenium release from the fuel. Concerning ruthenium transport in the reactor coolant system, recent experimental works[4,8,11,12] were devoted to better characterize deposits and gas phase of ruthenium oxides along a thermal gradient. All data indicate that a fraction of gaseous ruthenium is measured at the outlet, at quite a low temperature, about 150 °C, which may result from a direct formation in gas phase as well as some revaporization from Ru deposits onto surfaces. This gaseous fraction is attributed to $RuO_4$; the decomposition process of $RuO_4$ to $RuO_2$ seems to not be fast enough to reach the thermochemical equilibrium state as the rate of decomposition slows down with decreasing temperature. This behavior tends to indicate that a fraction of ruthenium can reach the nuclear containment building either under gaseous form or under

Received: February 17, 2015
Revised: April 23, 2015
Published: April 23, 2015





DOI: 10.1021/acs.jpca.5b01645
J. Phys. Chem. A 2015, 119, 4961−4971

aerosol form. The decomposition of $RuO_{4(g)}$ in moist air is quite slow; the half-life time of $RuO_4$ is found to be 5 h at 90 °C in the presence of steam.[2] All the recent literature information lead to the common conclusion that it is likely that some ruthenium can be released outside for some categories of severe accident involving a high oxidation of the fuel.

The modeling of ruthenium chemistry behavior in severe accident conditions can be performed using the ASTEC software package[16] (Accident Source Term Evaluation Code). This code requires trustful input data and accurate sets of thermodynamic properties [$\Delta_f H°(298\ K)$, $S°(298\ K)$, $C_p = f(T)$]. Usually, the reference values are taken from the works of Barin et al.,[15] Cordfunke and Konings,[13] and Garisto's;[14] they are listed in Tables 1 and 2. We hereafter present literature reviews of the origin of these data and the reported error bars.

**Table 1. Standard Enthalpies of Formation $\Delta_f H°(298\ K)$ in kJ mol$^{-1}$**

| species | Cordfunke and Konings[13] | Garisto[14] | Barin et al.[15] |
|---|---|---|---|
| $Ru_{(g)}$ | 649.0 ± 3.0 | 649.6 ± 13.0 | 651.4 |
| $RuO_{(g)}$ | 376 ± 25 | 372.0 ± 42.0 | |
| $RuO_{2(g)}$ | 136 ± 10 | 133.7 ± 15.0 | |
| $RuO_{3(g)}$ | −64.1 ± 2.5 | −48.4 ± 12.7 | −78.2 |
| $RuO_{4(g)}$ | −188.0 ± 0.4 | −187.1 ± 8.4 | −183.1 |

For $Ru_{(g)}$ standard enthalpy of formation, Cordfunke and Konings[13] made a third law recalculation using vapor pressure data measured by different authors either using mass spectrometry[17−19] or with the Langmuir method.[20] Out of these four references, they only retained the vapor pressure values of Panish and Magrave[17] and that of Carrera et al.,[18] proposing an average value 649.0 ± 3 kJ mol$^{-1}$. Garisto's[14] Ru heat of formation is directly taken from Rard,[21,22] who extended the reference data set with the mass spectrometry study of Krikorian et al.,[23] thus computing an average value of 649.6 ± 13.0 kJ mol$^{-1}$. Barin et al.[15] compiled very different reference data selected for solid and liquid Ru and, therefore, proposed a different value of 651.4 kJ mol$^{-1}$ for the standard enthalpy of formation at 298.15 K.

The standard enthalpy of formation of $RuO_{(g)}$, 376 ± 25 kJ mol$^{-1}$, has been obtained by Cordfunke and Konings from calculations of thermal functions using the vibrational frequencies of Pedley's review,[24] which in fact quotes the value derived by Norman et al.[19] by mass spectrometry. Garisto's accepted Pedley and Marshall's enthalpy of formation equal to 372.0 ± 42.0 kJ mol$^{-1}$.

As for $RuO_{(g)}$, Cordfunke and Konings estimated the thermal function of $RuO_{2(g)}$, taking the spectroscopic parameters of the analogous $MoO_{2(g)}$, to derive an enthalpy of formation of 136 ± 10 kJ mol$^{-1}$. Garisto's also used $MoO_{2(g)}$ spectroscopic parameters but taken from a different work.[25] Then he used Rard's[21,22] vapor pressure data to extract the enthalpy of formation equal to 133.7 ± 15.0 kJ mol$^{-1}$ at 298.15 K.

$RuO_3$ and $RuO_4$ are the two dominating gaseous species below 2000 K.[26] For the former, the reported value of −64.1 kJ mol$^{-1}$ by Cordfunke and Konings[13] proposed a value computed from an average of the measurements of Bell and Tagami,[26] Schäfer et al.,[27,28] and Alcok and Hooper.[29] Garisto's value of −48.4 ± 12.7 kJ mol$^{-1}$ is obtained by averaging the measurements of Bell and Tagami,[26] Schäfer et al.[27,28] and that of Rard.[21,22] The standard enthalpy value of −78.2 kJ mol$^{-1}$ listed in the compilation of Barin et al.[15] is taken from Glushko,[25] who in turn refers to earlier studies.[19,26−29]

Cordfunke and Konings calculated an average standard enthalpy of formation for $RuO_{4(g)}$ from the third law calculation from the data of Penman and Hammer,[30] Bell and Tagami[26] and Schäfer et al.,[27,28] with a larger weight on the data from Penman and Hammer.[30]

The uncertainties in the thermodynamic data arise mainly from the difficulties encountered while preparing the compounds. The use of highly correlated quantum chemical methods thus offers a promising way to provide these properties, as long as attention is paid to the accuracy of the quantum chemical method used because ruthenium is a transition metal and the electronic structure of some oxides could be quite complex as mentioned in Krauss and Stevens's work.[31] The main part of this paper consists in proposing an electronic structure methodology that offers a suitable accuracy within a reasonable computational cost. In this paper, we benchmark several quantum chemical methods for ruthenium oxide thermodynamic properties, for which experimental data are available, although sometimes with non-negligible uncertainties. The current investigation leads us to propose as an appropriate accuracy/computational time compromise the use of density functional theory (DFT) to obtain acceptable geometries and thermodynamic corrections with supplementary single-point energy calculations with post-HF approaches to obtain accurate electronic energies (correlation energies and/or spin−orbit coupling effects). This methodology can then be applied in forthcoming studies to explore other ruthenium species for which very few or no experimental data are available.

This article is organized as follows: the next section describes the computational methods and lists the set of chemical reactions considered here. It is followed by a discussion of the nature of ground states of the various oxides and of the Ru−O chemical bonds. Further down, we present the computed thermodynamic properties for Ru-containing species [$\Delta_f H°(298\ K)$, $S°(298\ K)$, and $C_p = f(T)$]. Our results are compared to available literature data.

**Table 2. Literature Values for the Standard Molar Entropies at 298 K [$S°(298\ K)$] and Heat Capacities at Constant Pressure [$C_p(298\ K)$] in kJ mol$^{-1}$ for the Gaseous Ruthenium Oxides**

| species | Cordfunke and Konings[13] | | Garisto[14] | | Barin et al.[15] | |
|---|---|---|---|---|---|---|
| | $S°(298\ K)$ | $C_p(298\ K)$ | $S°(298\ K)$ | $C_p(298\ K)$ | $S°(298\ K)$ | $C_p(298\ K)$ |
| $Ru_{(g)}$ | 186.4 | 21.5 | 186.4 ± 1 | / | 186.4 | 21.5 |
| $RuO_{(g)}$ | 242.1 | 31.5 | 242 ± 5 | / | 242.1 | |
| $RuO_{2(g)}$ | 267.4 | 44.1 | 283.9 ± 9 | 42.0 | 267.4 | |
| $RuO_{3(g)}$ | 281.9 | 59.4 | 291.4 ± 3.0 | 58.3 | 276.1 | 59.4 |
| $RuO_{4(g)}$ | 289.1 | 75.2 | 289.0 ± 1.0 | 75.1 | 290.1 | 75.6 |



DOI: 10.1021/acs.jpca.5b01645
J. Phys. Chem. A 2015, 119, 4961−4971

## COMPUTATIONAL DETAILS

**Electronic-Structure Calculations and Thermodynamic Corrections.** The structures of the various ruthenium containing species and other compounds that enter the formation reactions were optimized with Gaussian[32] with the default numerical integration grids. Specifying finer grids "Int (Grid=UltraFine)" lead to minor changes of the electronic energies (at most 2 kJ $mol^{-1}$). The ruthenium atom was described by a relativistic effective core potential (ECP28MDF)[33] with the corresponding augmented basis sets of triple-$\zeta$ quality.[33] The H and O atoms were described by the diffuse-augmented correlation consistent basis sets triple-$\zeta$ quality.[34]

Electron correlation is introduced in a comprehensive manner in usual density functional approximations (DFAs). In chemical systems for which the static correlation is negligible, hybrid functionals can generally describe the structural, electronic, and spectroscopic properties with an accuracy approaching that of the CCSD(T) method but with reduced computational cost. Indeed, the hybridization allows one to correct for the intrinsic self interaction error (SIE), which is problematic for the treatment of purely single-reference systems. However, the SIE could have a positive "involuntary" impact for systems with an avowed multireference character.[35−37] Thus, for such systems, it could be profitable to reduce hybridization toward pure (without HF exchange) DFAs. To ensure the best treatment of these multiconfigurational effects, the adjustment of the amount of hybridization has to be combined within a broken-symmetry treatment. Note that this might lead to wave functions that are not eigenfunctions of the $S^2$ operator, so that is the price to pay for DFT being a single-reference approach.

Using these arguments, a hybrid meta-GGA functional has been used. As our goal is to compute the enthalpies of reactions which include different complexes with different multireference characters, we suggest to use a moderated hybridization to reduce the errors on all geometrical parameters. At this stage, the TPSSh-5%HF functional[38] seems to comply with our expectations (note that the correlation part of the TPSS functional is self-interaction error free[38,39]). This choice will be discussed further down.

To discuss the accuracy of the electronic energies with respect to the treatment of electron correlation, and to investigate the potential multireference character of some ground state wave function, it was compulsory to explore other methods, in addition to the TPSSh-5%HF DFT values. Single and double coupled cluster theory with inclusion of a perturbative estimation for triple excitation [CCSD(T)] were performed with MOLPRO[40] with the spin-unrestricted open-shell coupled cluster theory for open-shell systems.[41,42] The computed $T_1$ diagnostics for the various species are 0.017, 0.054, 0.040, 0.034, and 0.035 for Ru, RuO, $RuO_2$, $RuO_3$, $RuO_4$, respectively. We observe the $T_1$ diagnostics for the oxide molecules are approaching the upper limit of 0.05 proposed for single-reference transition metal complexes.[43] This leads us to investigate the amount of nondynamical correlation in two complementary ways. Spin-contamination in broken-symmetry DFT calculations can be sought to quantify the multireference character. Spin-contamination appeared only in $RuO_2$ (40%). Another diagnostic of MR character is provided by the weight $C_0^2$ of the leading configuration in a multireference calculation. Full valence (oxygen 2s and 2p and ruthenium 5s and 4d) CASSCF and post-CASSCF calculations were computationally feasible for Ru, RuO, and $RuO_2$ with MOLPRO.[40] The post-CASSCF treatment of dynamical correlation was performed with (1) a variational multireference singles plus doubles configuration interaction calculation (MRCI) with the Davidson's size-consistent correction,[44] (2) the perturbative CASPT2[45,46] using the ionization potential electron affinity (IPEA) corrected zeroth-order Hamiltonian,[47] and (3) the quasi-degenerate partially contracted $n$-electron valence states second-order perturbation theory scheme (QD-PCNEVPT2).[48] The computed $C_0^2$ are larger than 0.9, confirming that despite the relatively large $T_1$ values,[43] the ground-state wave functions have a negligible multireference character.

We have also estimated the influence of spin−orbit coupling for the open-shell systems Ru and RuO but also for $RuO_2$ for which a triplet state is close to the singlet ground state, by performing a spin−orbit coupled state-interaction calculation as implemented in MOLPRO.[40] The spin−orbit contribution to the total Hamiltonian was computed from the integrals of the ruthenium spin−orbit pseudopotential operator.[33] For Ru, we coupled 15 quintet, 36 triplet, and 36 singlet states spanned by the full-valence active space discussed in the previous paragraph. For RuO, we considered the seventh lowest-lying state of each spin multiplicity (singlet, triplet, and quintet), while for $RuO_2$, we considered the first 20 states of each spin multiplicity, that is states within a 2 eV energy window.

At all levels of correlation (TPSSh-5%HF, CCSD(T), MRCI +Q, CASPT2, QD-NEVPT2), we performed single-point calculations with basis sets of triple, quadruple, and quintuple zeta quality ($n$ = 3−5). The corresponding Hartree−Fock or CASSCF $E_{HF/CASSCF}$ and correlation $E_{corr}$ energy components were used to extrapolate the complex total energies to their complete basis set (CBS) limit using a three-point exponential formula for $E_{HF/CASSCF}$:[49,50]

$$E_{HF/CASSCF}(n) = E_{HF/CASSCF}^{CBS} + A\exp(-Bn) \quad (1)$$

and a two-point extrapolation for $E_{corr}$[51]

$$E_{corr}(n) = E_{corr}^{CBS} + An^{-3} \quad (2)$$

Natural population analysis (NPA) were carried out with Gaussian.[32] The topological analysis was performed with the AIMall package.[52]

**Chemical Reactions Used to Derive the Standard Enthalpies for Formation of RuO and $RuO_2$.** To obtain the standard enthalpy of formation of RuO and $RuO_2$, we will use the known standard enthalpy of formation of Ru (See Table 1), together with the enthalpies of reactions of the following four formation reactions:

$$R_1(n)\text{: Ru} + n\text{O} \rightarrow \text{RuO}_n \quad (3)$$

$$R_2(n)\text{: Ru} + n\frac{1}{2}\text{O}_2 \rightarrow \text{RuO}_n \quad (4)$$

$$R_3(n)\text{: Ru} + n\text{HO} \rightarrow \text{RuO}_n + n\text{H} \quad (5)$$

$$R_4(n)\text{: Ru} + n\text{H}_2\text{O} \rightarrow \text{RuO}_n + n\text{H}_2 \quad (6)$$

The values of the standard enthalpies of formation for H, $H_2$, $H_2O$, HO, O, and $O_2$ have been taken from the literature[53] and are listed in Table S1 of the Supporting Information.

We can also derive the target enthalpies making use of the known standard enthalpies of formation of $RuO_4$ (See Table 1)



DOI: 10.1021/acs.jpca.5b01645
J. Phys. Chem. A 2015, 119, 4961−4971

Table 3. Calculated Born-Oppenheimer Equilibrium Distance ($r_e$) and Zero-Point Average Distance ($r_0$) in RuO Computed with Various Density Functional Approximation (DFA) (Bond Lengths in Å and Angles in Degrees)[a]

| | | | | TPSSh-X%HF | | | |
|---|---|---|---|---|---|---|---|
| coordinate | M06-L | M11-L | SOGGA-11 | 0% | 10% | 5% | exp |
| $r_e$ | 1.721 | 1.712 | 1.706 | 1.718 | 1.709 | 1.713 | 1.716[54] |
| $r_0$ | 1.725 | 1.716 | 1.710 | 1.721 | 1.713 | 1.717 | 1.70[55] |

[a]Comparison to experimental data.

and of the computed enthalpies of dissociation for the four following chemical reactions:

$$R_1(m, n) \quad : \quad RuO_m \rightarrow RuO_n + (m - n)O \tag{7}$$

$$R_2(m, n) \quad : \quad RuO_m \rightarrow RuO_n + (m - n)\frac{1}{2}O_2 \tag{8}$$

$$R_3(m, n) \quad : \quad RuO_m + (m - n)H \rightarrow RuO_n + (m - n)HO \tag{9}$$

$$R_4(m, n) \quad : \quad RuO_m + (m - n)H_2 \rightarrow RuO_n + (m - n)H_2O \tag{10}$$

This reaction set will be also used to compute the standard enthalpy of formation of Ru, which can be directly compared to literature values (see Table 1), thus providing not only a direct validation of the reaction schemes but also an assessment of the accuracy of the electronic structure approaches.

## RESULTS AND DISCUSSION

The present discussion of the results is divided into three subsections. In the first subsection, we discuss the accuracy of TPSSh for the geometrical parameters and vibrational frequencies and we analyze the electronic structure of the various ruthenium oxides. The second section is devoted to the analysis of the Ru−O chemical bonds. In the third subsection, we will discuss the computed thermodynamic parameters.

**Geometries, Vibrational Frequencies, and Electronic Structures of the Ruthenium Species.** *Choice of a Suitable DFA for Geometrical Parameters and Vibrational Frequencies.* In Table 3 and Table S2 of the Supporting Information, we compare the geometries of the ruthenium monoxide (both $r_e$ and $r_0$) and the reactive species in Reactions 3,4,5, and 6 obtained with TPSSh-5%HF with that obtained with other DFA and to experimental data. While the M11-L and SOGGA-11 were chosen by Li et al.[56] for their study on iron carbide reactivity, they lead for our systems to slightly too short bond lengths in comparison to experiment. We can notice that TPSSh-5%HF functional is the most accurate, thus all geometries and frequencies discussed hereafter are obtained at this level of theory.

*Ru Atom.* At the spin−orbit free level, the ground state of the ruthenium atom is expected to be a $^5F$, corresponding to the electronic configuration $5s^14d^7$. Spin−orbit coupling (SOC) not only lifts the degeneracy of that state but also mixes it with the higher lying atomic states, giving rise to a dense atomic spectrum, out of which we only report in Table 4 the first five $J$ levels to discuss the accuracy of the treatment of correlation effects and SOC. The first four excitation energies agree well with the experimental values, indicating that there is a weak interplay between electron correlation and SOC and that the SOC has been accurately treated by the spin−orbit effective core potential. All levels predict that SO contribution to the ruthenium atom, taken as the difference between the $J$ = 5 spin−orbit ground state and the $^5F$ spin−orbit free ground state amounts to 16 kJ mol$^{-1}$.

Table 4. Excitation Energies (cm$^{-1}$) and Mean Signed Error MSE with Respect to the Experimental Data of the First Five $J$ Levels of Ru[a]

| configuration | $J$ | SO-MRCI +Q | SO-CASPT2 | SO-QDNEVPT2 | exp[57] |
|---|---|---|---|---|---|
| $4d^7(a^5F)5s$ | 5 | 0 | 0 | 0 | 0 |
| | 4 | 1022 | 1187 | 1078 | 1191 |
| | 3 | 1849 | 2023 | 1904 | 2092 |
| | 2 | 2548 | 2691 | 2486 | 2713 |
| | 1 | 2874 | 2986 | 2853 | 3105 |
| MSE | | −161 | −20 | −153 | |

[a]Spin-orbit free correlated energies obtained at the MRCI+Q, CASPT2, or QD-NEVPT2 levels are used to dress the state-interaction SOC matrix.

*RuO.* Krauss and Stevens[31] were the first to examine the electronic structure of RuO with multiconfigurational SCF calculations and predicted the ground state to be a $^5\Delta$. Like Zhou et al.,[58] this is also what we obtain both in the DFT and in the multiconfigurational wave function calculations. The latter confirms that the wave function is well-described by a single open-shell Slater determinant. The Ru−O bond is short, 1.713 Å, with a stretching vibrational frequency of 895 cm$^{-1}$, signs of a strong covalent bond as described in the bonding section. Table S3 of the Supporting Information summarizes the computed spin−orbit contributions that amount to −10.46, −10.42, and −10.60 kJ mol$^{-1}$, at the SO-CASPT2, SO-MRCI +Q, and SO-CASSCF levels, respectively.

*$RuO_2$.* All calculations reported so far on $RuO_2$,[58−60] just like ours, predict a singlet $A_1$ ground state for $RuO_2$, with a wave function dominated by one closed-shell Slater determinant. However, we noticed that, at the CASSCF level, the lowest triplet states of $A_1$ and $B_1$ symmetries lie only 4 kJ mol$^{-1}$ above the singlet $A_1$ state. At the SO-CASSCF level, SOC splits the components of the low-lying triplets $A_1$ and $B_1$, pushing them below the spin−orbit state that has a strong $^1A_1$ component, as illustrated by the low-lying transition energies computed at the SOC level listed in Table 5. This change of ground-state character does not occur when dynamical electron correlation is included, as the latter stabilizes more the singlet-state energy than that of the triplet state, leading to larger values of the singlet−triplet gaps, with values of 29.2, 38.8, 55.6, and 24.8 kJ mol$^{-1}$ at the CASPT2, MRCI, CCSD(T), and TPSSh-5%HF levels of theory, respectively. The spin−orbit energetic stabilization of the $RuO_2$ is equal to 0.73 and 0.70 kJ mol$^{-1}$, respectively, for the SO-CASPT2 and SO-MRCI+Q levels. At the SO-CASSCF level, this stabilization is estimated to 1.6 kJ mol$^{-1}$, a value that agrees with the SO-CASPT2 and SO-MRCI +Q values. Note that this contribution is extremely small as one



DOI: 10.1021/acs.jpca.5b01645
J. Phys. Chem. A 2015, 119, 4961−4971

Table 5. Excitation Energies in $cm^{-1}$ of the Low-Lying Energy Levels of $RuO_2$ Computed at the SO-CASSCF, SO-CASPT2, and SO-MRCI+Q Levels of Theory

| composition | SO-CASSCF | composition | SO-MRCI+Q | composition | SO-CASPT2 |
|---|---|---|---|---|---|
| 51% $^3A_1$ + 49% $^3B_1$ | 0 | 99% $^1A_1$ | 0 | 99% $^1A_1$ | 0 |
| 52% $^3A_1$ + 48% $^3B_1$ | 1 | 48% $^3A_1$ + 52% $^3B_1$ | 3163 | 52% $^3A_1$ + 48% $^3B_1$ | 1649 |
| 62% $^1A_1$ + 40% $^3B_1$ | 653 | 48% $^3A_1$ + 52% $^3B_1$ | 3164 | 52% $^3A_1$ + 48% $^3B_1$ | 1650 |
| 99% $^3A_1$ | 732 | 99% $^3B_1$ | 3871 | 99% $^3A_1$ | 2361 |
| 38% $^1A_1$ + 62% $^3B_1$ | 856 | 98% $^3A_1$ | 3942 | 98% $^3B_1$ | 2425 |

might expect for an electronic state with a major singlet character. At this stage, we can conclude that the SO-CASSCF approach allows us to accurately estimate the energetic contribution of spin−orbit coupling for Ru, RuO, and $RuO_2$, compared to SO-CASPT2 and SO-MRCI+Q methods. The spin−orbit contributions are listed in Table S3 of the Supporting Information.

As discussed by Hameka et al.[59] and Siegbahn,[60] the $RuO_2$ molecule is bent as a result of the interaction between the oxygen lone pairs and empty, or half-empty, 4d ruthenium orbitals. The TPSSh-5%HF geometry (1.685 Å, 149.8°) is close to the geometries optimized at the Hartree−Fock level (1.595 Å, 150.6°)[59] and at the B3LYP level (1.697 Å, 152.4°)[58] (See Table 6). The computed O−Ru−O angle is close to the value of 148 ± 2° predicted by Kay et al.[61] Our calculations place the symmetric stretching frequency, 972 $cm^{-1}$, above the antisymmetric stretching one, 964 $cm^{-1}$. B3LYP calculations predict these vibrational modes at 990.1 and 989.7 $cm^{-1}$. Both TPSSh-5%HF and B3LYP values are about 50 $cm^{-1}$ larger than that measured by Kay et al. in an argon matrix (926 and 902 $cm^{-1}$). Zhou et al.[58] only observed the antisymmetric stretching mode at 918.4 and 905.1 $cm^{-1}$ in neon and argon matrices, respectively. We predict a larger split between the two modes that computed at the B3LYP level.[58] Note that with the BP86 density functional, the antisymmetric vibration is higher than the symmetric one. The possibility of having an inversion of the two frequencies indicates that the description of the Ru−O bonds is very sensitive to electron correlation.

Table 6. Bond Distances (Å), O−Ru−O Angles ($\theta$, deg), and Vibrational Frequencies ($cm^{-1}$), and Infrared Intensities ($km\ mol^{-1}$) in Parentheses for the Ru Oxides

| species | method | r, θ | frequencies (intensity) |
|---|---|---|---|
| RuO ($^5\Delta$; $C_{\infty v}$) | TPSSh-5% HF[a] | 1.713 | 895.0 (133) |
| | B3LYP[b] | 1.745 | 862.7 (130) |
| | MCSCF[c] | 1.740 | 814 (−) |
| $RuO_2$ ($^1A_1$; $C_{2v}$) | TPSSh-5% HF[a] | 1.685, 149.8 | 972.4 ($a_1$, 5); 964.3 ($b_2$, 358); 191.7 ($a_1$, 21) |
| | B3LYP[b] | 1.697, 152.4 | 990.1 (8); 989.7 (466); 206.1 (35) |
| | HF[d] | 1.595, 150.6 | 1098 (21); 817 (816); 307 (55) |
| $RuO_3$ ($^1A_1'$; $D_{3h}$) | TPSSh-5% HF[a] | 1.687 | 963.9 (0); 963.0 (264); 298.2 ($e'$, 2); 71.3 ($a_2''$, 71) |
| | BP86[e] | 1.717 | 949.7 (125); 948.0 (125); 915.8 (0); 289.8 (1); 289.7 (1); 77.5 (9) |
| | HF[d] | 1.610 | 1055(0); 759 (146); 330 (13); 185 (27) |
| $RuO_4$ ($^1A_1$; $T_d$) | TPSSh-5% HF[a] | 1.691 | 974.3 ($t_2$, 254); 952 ($a_1$, 0), 350 ($t_2$, 2154); 327 ($e$, 0) |
| | BP86[e] | – | 950.2 (100); 904.0 (0) |
| | HF[d] | 1.608 | 1066(0); 923 (273); 413 (22); 398 (0) |

[a]This work. [b]Ref 58. [c]Ref 31. [d]Ref 59. [e]Ref 58 with BP86 functional.

*$RuO_3$ and $RuO_4$ Species.* $RuO_3$ and $RuO_4$ both have singlet ground states. Broken symmetry calculations did not exhibit any spin contamination, ensuring that these states are well-described by a single closed-shell determinant; this is further confirmed by the analysis of the ground-state wave function. At the Hartree−Fock level and using large-core relativistic effective core potentials, Hameka et al.[59] found a singlet ground state for both species. However, using relativistic all-electron basis sets and a relativistic Hamiltonian at first-order of the perturbation theory including the mass-velocity and Darwin terms, Siegbahn[60] found triplet ground states for both species, but at the correlated level, the singlet states turned out to be lower in energy. We confirmed that by optimizing geometries for the lowest triplet state at the TPSSh-5%HF level and found in both cases a significant gap between the lower singlet state and the triplet state of 62 and 170 kJ $mol^{-1}$ for $RuO_3$ and $RuO_4$, respectively.

Garisto proposed a $C_{3v}$ pyramidal structure for $RuO_3$, but our geometry optimization leads to planar with a $D_{3h}$ symmetry as found by Siegbahn[60] and Zhou et al.[58] Our computed antisymmetric frequency is at 963 $cm^{-1}$, slightly larger than that computed at the B3LYP level, 948.0 $cm^{-1}$, or that measured experimentally at 893.4 $cm^{-1}$ in argon matrix[61] and 901.1 $cm^{-1}$ in neon matrix.[58] $RuO_4$ has a tetrahedral structure. Infrared measurements in solid argon assigned a band at 916.9 $cm^{-1}$ to the $t_2$ mode. In neon, that band is measured at 923.0 $cm^{-1}$, while DFT calculations place it at higher values, 974.2

Table 7. Ru−O Bond Distances, Natural Population Analysis (NPA) Charges, and Bond Critical Points (BCP) Parameters: $\rho_b$ and $\nabla^2\rho_b$ are the electron density and the Laplacian at the BCP given in $e^-/bohr^3$ and $e^-/bohr^5$[a]

| species | $r_e$ (Å) | q(Ru) | q(O) | δ(Ru,O) | $\rho_b$ ($e^-/bohr^3$) | $\nabla^2\rho_b$ ($e^-/bohr^5$) | $H_b$ (au) |
|---|---|---|---|---|---|---|---|
| RuO ($^5\Delta$, $C_{\infty v}$) | 1.713 | 0.62 | −0.62 | 2.25 | 0.24 | 0.76 | −0.153 |
| $RuO_2$ ($^1A_1$; $C_{2v}$) | 1.685 | 0.99 | −0.49 | 1.93 | 0.26 | 0.91 | −0.174 |
| $RuO_2$ ($^3B_1$; $C_{2v}$) | 1.686 | 0.99 | −0.50 | 2.01 | 0.26 | 0.93 | −0.172 |
| $RuO_3$ ($^1A_1'$; $D_{3h}$) | 1.687 | 0.99 | −0.33 | 1.89 | 0.27 | 0.94 | −0.173 |
| $RuO_4$ ($^1A_1$; $T_d$) | 1.691 | 1.05 | −0.26 | 1.68 | 0.27 | 0.83 | −0.175 |

[a]δ(Ru,O) is the delocalization index. $H_b$ (au) is the energy density at the critical point.



DOI: 10.1021/acs.jpca.5b01645
J. Phys. Chem. A 2015, 119, 4961−4971

$cm^{-1}$ from our results (See Table 6), and 950.2 $cm^{-1}$ with the BP86 functional.[58]

**Nature of the Ru−O Chemical Bonds in the Ruthenium Oxides.** We will now discuss the nature Ru−O chemical bonds in the ruthenium oxides using two viewpoints: (i) the bonding molecular orbital picture; (ii) a quantitative analysis of the topology of density in the interatomic region. The later relies on the quantum theory of atoms-in-molecules (QTAIM),[62,63] which characterizes and classifies chemical bonding interactions according to the properties of the electron density $\rho_b$, its Laplacian $\nabla^2\rho_b$, and the energy density $H_b$ (sum of the kinetic $G$ and potential $V$ energy densities) at the bond critical point (BCP), corresponding to the point of lowest electron density between two bonded atoms.[64] Typically, value of $\rho_b$ greater than 0.2 $e^-/bohr^3$ are found for covalent interactions, while values of $\rho_b < 0.1e^-/bohr^3$ indicate closed shell interactions. $H_b$ is negative for interactions with significant sharing of electrons, its magnitude reflecting the covalence of the interaction.[65] Table 7 presents these QTAIM parameters for the various ruthenium oxides, together with the delocalization index $\delta$(A, B), which can be viewed as a measure of the bond order between atoms A and B.

For all oxides, the QTAIM data suggest that the Ru−O bonds are strong covalent bonds, since $\rho_b > 0.24$, and $H_b$ is negative. These two quantities are nearly constant across the series of oxides. The delocalization index is larger than 2 for RuO, while it is lower than 2 and smoothly decreases to 1.68 as higher oxidation states oxides are formed.

The molecular orbitals involved in forming RuO are depicted in the Figure 1 (panels a−e), together with the occupation

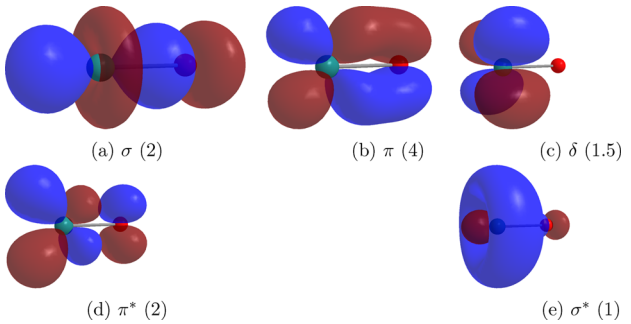


**Figure 1.** DFT (TPSSh-5%HF) molecular orbitals forming the chemical bond between ruthenium (on the left) and oxygen (on the right) in RuO. The orbital label is given below each orbital, together with the number of electrons occupying this orbital or pair of orbitals in the case of degeneracy. Red is for negative charges and blue for positives charges.

number of each orbital (or pair of orbitals). As illustrated in the figure, the lowest-energy doubly occupied molecular orbital can be viewed as a single $\sigma$ bond involving the ruthenium $4d_\sigma$ and oxygen $2p_z$ orbitals. The other two doubly occupied orbitals are degenerate of covalent $\pi$ type and result from the combination of the ruthenium $4d_\pi$ and oxygen $2p_{x,y}$ orbitals. The two doubly degenerate $4d_\delta$ orbitals are purely localized on the ruthenium atoms. They carry a total of 1.5 electrons, indicating that one $\delta$ component is doubly occupied, while the other one is singly occupied in the two spatially degenerate components of the $^5\Delta$. The remaining three unpaired electrons occupy the antibonding $\pi^*$ orbitals, and the ruthenium 5$s$ orbital. Overall, our calculation indicates that RuO has three electron-pair bonds, although the delocalization index claims a bond order of 2.3 (See Table 7). This situation resembles to the one U−O triple bonds in the uranyl $UO_2^{2+}$ molecules, which are assigned bond orders of the order of 2.1−2.3.[66,67]

Like in RuO, ruthenium in $RuO_2$ forms strong and short bonds to the two neighboring oxygen atoms. On Figure 2 (panels a to h) are depicted the highest occupied molecular orbitals that have a bonding character. The first five molecular orbitals correspond to $\sigma$ and $\pi$ bonds involving the ruthenium 4d and oxygen 2p orbitals. The last orbital is nonbonding as there is no overlap between the ruthenium $4d_\delta$ and the oxygen 2p orbitals. Summing up the number of bonding orbitals, we conclude that RuO has 2.5 electron-pair bonds. Since there are also antibonding orbitals being doubly occupied (not depicted here), we can estimate the bond order to be close to 2, as also estimated by the delocalization index in Table 7. As the first triplet state $^3B_1$ state is close in energy to the $^1A_1$ ground state, it is interesting to analyze its density. The two unpaired electrons occupy two essentially nonbonding orbitals shown in Figure 2 (panels g and h), suggesting that the Ru−O bonds are identical to that of the singlet state. This observation is supported by the very similar QTAIM parameters between the $^3B_1$ and $^1A_1$ states.

In $RuO_3$, we can count a total of six bonding orbitals illustrated in Figure 3 (panels a to f), making up three Ru═O double bonds, quite close to the $\delta$(A,B) value of 1.83. In $RuO_4$, this value drops down to 1.68. In that system, we can list only five bonding orbitals shown in Figure 4 (panels a to e), making up an average bond order of 1.25.

An alternative way of quantifying bond strength is to look at the reactions $RuO_n \rightarrow RuO_{n-1} + O$ ($n$ = 1−4), corresponding to the stepwise bond dissociation energies. Using the modified coupled-pair functional correlated method and neglecting spin−orbit coupling, Siegbahn[60] reported monotonically decreasing bond strengths. Our CCSD(T) values listed in Table 8[60] lead to a different picture, indicating that the Ru−O bond strength reaches a maximum for $RuO_2$ and decreases when additional oxygen atoms bind ruthenium. However, this decreases in the strength of the Ru−O bond is not mirrored in the Ru−O bond distances that do not vary, while one would expect a lengthening of the interatomic distance when the bond order decreases. The natural population charges reported in Table 7 indicate that, the higher the oxidation state, the more ruthenium is positively charged, thus enhancing the purely electrostatic interactions with the neighboring oxygens. This effect should result in a shortening of the bond that counterbalance for the decreasing covalent character. The sum of these two competing effects keeps the Ru−O distance constant in the $RuO_n$ species.

**Calculation of Standard Enthalpy of Formation.** To validate the accuracy of the methods, we have first made use of the literature standard enthalpies of formation of $RuO_4$, which have very low uncertainty to derive the corresponding values for the other oxides. The oxides $RuO_3$ and $RuO_4$ have closed-shell ground states and are thus well-described by a single determinant, making coupled-cluster CCSD(T) methods applicable. In the case of Ru and RuO, which have an open-shell ground state, we converged the wave function at the restricted open-shell (ROHF) level, choosing one of the degenerate determinants of the $^5F$ or $^5\Delta$, respectively. At the DFT level, the lowest state of $RuO_2$ is an unrestricted singlet open-shell state. We have performed both CCSD(T) and U-CCSD(T) (using the guess from DFT broken-symmetry


DOI: 10.1021/acs.jpca.5b01645
J. Phys. Chem. A 2015, 119, 4961−4971

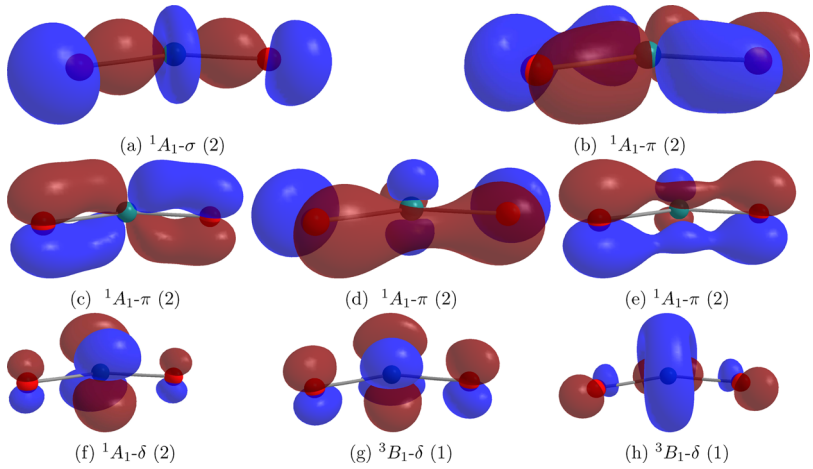


**Figure 2.** DFT (TPSSh-5%HF) forming the chemical bond between ruthenium (at the center) and the two oxygen atoms in $RuO_2$ in the $^1A_1$ ground state (a–f) and in the singly occupied orbitals in the $^3B_1$ orbital (g–h). The orbital label is given below each orbital and the occupation number in parentheses.

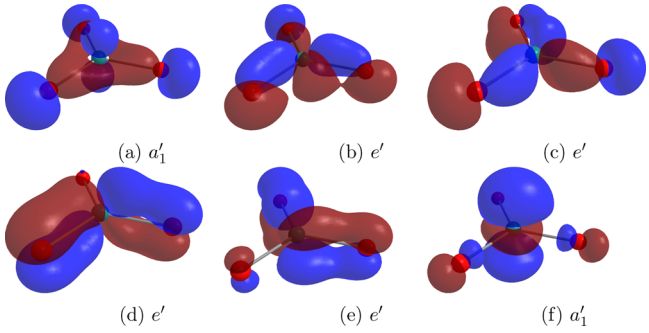


**Figure 3.** DFT (TPSSh-5%HF) doubly occupied molecular bonding orbitals in $RuO_3$. Their symmetry is given below each orbital.

calculation) and found that the closed-shell CCSD(T) provides a lower total energy.

Making use of the experimental standard enthalpy of formation of $RuO_4$, we can derive the $\Delta_f H°(298\ K)(RuO_3)$ value from the four reactions $R_1(3, 4)$, $R_2(3, 4)$, $R_3(3, 4)$, and $R_4(3, 4)$. The resulting $\sigma$-value is lower than the usual energetic uncertainties obtained with a high level quantum chemistry method which is about 4 kJ mol$^{-1}$. As shown in Table 9, all four reactions lead to very similar values for that enthalpy, with an average of $-50.7 \pm 0.5$ kJ mol$^{-1}$. Our value differs by about 14 kJ mol$^{-1}$ from the literature value, $-64.1 \pm 2.5$ kJ mol$^{-1}$ derived by Cordfunke and Konings.[13] Zimmerman et al.,[68] who had made independent estimated thermodynamic properties for gaseous Ru oxides compounds using additional knowledge of structures and vibrational frequencies obtained from their low-temperature matrix studies[61,69] and using also Norman et al.[19] thermochemical data, found for $\Delta_f H°(298\ K)(RuO_3)$ $-58 \pm 4$ kJ mol$^{-1}$, a value that differs from ours by about 8 kJ mol$^{-1}$.

**Table 8. Stepwise Binding Energies $-\Delta E_{n-1,n}$ and Binding Enthalpies at 298 K in kJ mol$^{-1}$ of Oxygen to Ruthenium Oxide $Ru_{n-1}$, for Reaction $RuO_{n-1} + O \rightarrow RuO_n$, Computed at the CCSD(T) Level, Using TPSSh5%HF Geometries**

| | $n = 1$ | $n = 2$ | $n = 3$ | $n = 4$ |
|---|---|---|---|---|
| $-\Delta E_{n-1,n}$ | 481 | 532 | 443 | 385 |
| $-\Delta E_{n-1,n}$ | 421 | 379 | 355 | 270 |
| $-\Delta H_{n-1,n}$ (298 K) | 472 | 528 | 440 | 384 |

Using either the standard enthalpy of formation computed at the CCSD(T) level for $RuO_3$ or the experimental value for $RuO_4$, we derive either way a standard enthalpy of formation of Ru, RuO, and $RuO_2$, considering the average over the four listed formation reactions. For Ru, we recommend a value of $638 \pm 2$ kJ mol$^{-1}$, about 10 kJ mol$^{-1}$ lower than the experimental value ($649 \pm 3$ kJ mol$^{-1}$). Zimmerman[68] calculated that the standard enthalpy of formation equal to $640 \pm 4$ kJ mol$^{-1}$ is in good agreement with our recommended value. In the case of RuO, we propose a value of $420.3 \pm 1.3$ kJ mol$^{-1}$, which is 44 kJ mol$^{-1}$ higher than currently accepted experimental values of $376 \pm 25$ kJ mol$^{-1}$, whereas Zimmerman obtained $376 \pm 4$ kJ mol$^{-1}$. For $RuO_2$, the average CCSD(T) value, $140.2 \pm 1.0$ kJ mol$^{-1}$, falls in the range of the uncertainty of the experimental value, $136 \pm 10$ kJ mol$^{-1}$, similar to the Zimmerman value of $140 \pm 4$ kJ mol$^{-1}$.

Since Ru and RuO species have open-shell ground states, we decided to compare the results of CCSD(T) to that obtained from multireference correlated calculations, for $\Delta_f H°(298\ K)$ of RuO and $RuO_2$, using the known value of the experimental $\Delta_f H°(298\ K)$ for Ru. The results are summarized in Table 10. Focusing first on the results obtained with CCSD(T), the standard enthalpy of formation of RuO is $431.0 \pm 0.5$ kJ mol$^{-1}$, and that of $RuO_2$, $151.0 \pm 1.0$ kJ mol$^{-1}$, both 10 kJ mol$^{-1}$

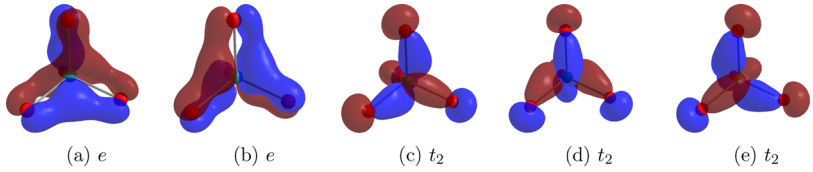


**Figure 4.** DFT (TPPSh-5%) doubly occupied molecular bonding orbitals in $RuO_4$. Their symmetry is given below each orbital.



DOI: 10.1021/acs.jpca.5b01645
J. Phys. Chem. A 2015, 119, 4961–4971

**Table 9. Standard Enthalpies of Formation for Ru, RuO, $RuO_2$, $RuO_3$ in kJ $mol^{-1}$ Computed at the CCSD(T) Level of Theory for the Various Reactions $R_m(n,4)$ ($m$ = 1,4, $n$ = 0−3), Using TPSSh-5%HF Optimized Geometries and the Experimental Standard Enthalpy of Formation of $RuO_4$.$\overline{\Delta_f H^\circ}$(298 K) ± $\sigma$ Represents the Average and the Standard Deviation of Computed Standard Enthalpies of formation[a]**

| Ru | $\Delta_f H^\circ$(298 K)lit =649 ± 3 kJ $mol^{-1}$ | | | | |
|---|---|---|---|---|---|
| from $RuO_4$ | $R_1(0,4)$ | $R_2(0,4)$ | $R_3(0,4)$ | $R_4(0,4)$ | $\overline{\Delta_f H^\circ}$ (298 K) ± $\sigma$ |
| UCCSD(T) | 638.0 | 641.4 | 639.5 | 634.6 | 638.4 ± 2.1 |
| RuO | $\Delta_f H^\circ$(298 K)lit =376 ± 25 kJ $mol^{-1}$ | | | | |
| from $RuO_4$ | $R_1(1,4)$ | $R_2(1,4)$ | $R_3(1,4)$ | $R_4(1,4)$ | $\overline{\Delta_f H^\circ}$ (298 K) ± $\sigma$ |
| UCCSD(T) | 420.1 | 422.7 | 421.3 | 417.6 | 420.4 ± 1.6 |
| $RuO_2$ | $\Delta_f H^\circ$(298 K)lit =136 ± 10 kJ $mol^{-1}$ | | | | |
| from $RuO_4$ | $R_1(2,4)$ | $R_2(2,4)$ | $R_3(2,4)$ | $R_4(2,4)$ | $\overline{\Delta_f H^\circ}$ (298 K) ± $\sigma$ |
| CCSD(T) | 140.1 | 141.8 | 140.8 | 138.3 | 140.3 ± 1.0 |
| $RuO_3$ | $\Delta_f H^\circ$(298 K)lit = −64.1 ± 2.5 kJ $mol^{-1}$ | | | | |
| from RuO4 | $R_1(3,4)$ | $R_2(3,4)$ | $R_3(3,4)$ | $R_4(3,4)$ | $\overline{\Delta_f H^\circ}$ (298 K) ± $\sigma$ |
| CCSD(T) | −50.8 | −49.9 | −50.4 | −51.6 | −50.7 ± 0.5 |

[a]The literature values are taken from Cordfunke and Konings[13].

**Table 10. Computed Standard Enthalpies of Formation for RuO and $RuO_2$ Obtained at the DFT and CCSD(T) Levels for the Various Reactions $R_m(n)$ ($m$ = 1−4, $n$ = 1−2), and with Multi-Reference Correlated Calculations Using TPSSh-5%HF Optimized Geometries[a]**

| RuO | $\Delta_f H^\circ$(298 K)lit =376 ± 25 kJ $mol^{-1}$ (ref 13) | | | | |
|---|---|---|---|---|---|
| from Ru | $R_1(1)$ | $R_2(1)$ | $R_3(1)$ | $R_4(1)$ | $\overline{\Delta_f H^\circ}$ (298 K) ± $\sigma$ |
| TPSS | 392.1 | 397.4 | 391.4 | 362.7 | 385.9 ± 11.6 |
| TPSSh-5%HF | 410.7 | 418.1 | 407.5 | 377.8 | 403.5 ± 12.8 |
| TPSSh-10%HF | 429.0 | 420.6 | 423.3 | 392.6 | 416.4 ± 11.9 |
| MRCI+Q | 476.3 | 470.7 | 473.0 | 468.1 | 472.0 ± 2.6 |
| CASPT2 | 407.8 | 418.4 | 406.6 | 406.8 | 409.9 ± 4.2 |
| QDNEVPT2 | 381.2 | 397.3 | 387.7 | 398.3 | 391.1 ± 6.7 |
| CCSD | 489.5 | 468.9 | 481.9 | 475.4 | 478.9 ± 6.8 |
| CCSD(T) | 431.1 | 430.3 | 430.7 | 432.0 | 431.0 ± 0.5 |
| $RuO_2$ | $\Delta_f H^\circ$(298 K)lit =136 ± 10 kJ $mol^{-1}$ (ref 13) | | | | |
| from Ru | $R_1(2)$ | $R_2(2)$ | $R_3(2)$ | $R_4(2)$ | $\overline{\Delta_f H^\circ}$ (298 K) ± $\sigma$ |
| TPSS | 107.1 | 135.5 | 105.8 | 48.4 | 99.2 ± 25.4 |
| TPSSh-5%HF | 147.3 | 162.1 | 140.9 | 81.6 | 133.0 ± 25.7 |
| TPSSh-10%HF | 186.7 | 188.3 | 175.3 | 114.1 | 166.1 ± 26.0 |
| MRCI+Q | 196.9 | 185.7 | 190.4 | 180.6 | 188.4 ± 5.2 |
| CASPT2 | 75.0 | 96.1 | 72.7 | 73.0 | 79.2 ± 8.5 |
| QDNEVPT2 | 24.0 | 56.3 | 36.9 | 58.1 | 43.8 ± 13.4 |
| CCSD | 309.9 | 268.8 | 294.8 | 281.7 | 288.8 ± 13.6 |
| CCSD(T) | 151.1 | 149.5 | 150.4 | 152.8 | 151.0 ± 1.0 |

[a]$\overline{\Delta_f H^\circ}$ (298 K) ± $\sigma$ represents the average and the standard deviation of computed standard enthalpies of formation.

higher than the values derived using the experimental standard enthalpy of formation for $RuO_4$.

It is noteworthy that the variational (MRCI+Q) and perturbative (CASPT2, or QD-NEVPT2) yield $\Delta_f H^\circ$(298 K) values that differ quite significantly from the CCSD(T) values. We have tried to enlarge the orbital active space by adding one shell of ruthenium $d$ orbitals. This results in very large active spaces, which could only be handled for Ru and RuO but turned out to be far too large (about 300 millions CSFs) for $RuO_2$. These larger active spaces yielded changes the formation enthalpy of RuO from 488.5 ± 4.6 kJ $mol^{-1}$ down to 433.5 ± 4.6 kJ $mol^{-1}$ with the MRCI+Q method, and from 443.3 ± 6.3 to 447.4 ± 6.3 kJ $mol^{-1}$, with the CASPT2 method, both very close to the CCSD(T) value. It is also worth pointing out the sizable contribution of triple excitations measured by the differences between the CCSD and CCSD(T) results for RuO and $RuO_2$ $\Delta_f H^\circ$(298 K) (See Table 10). This together with the need for very large active space in multireference calculations highlights the fact that ruthenium oxides are strongly correlated molecules.

We have also investigated the accuracy of the TPSSh DFA with 0, 5, or 10% Hartree−Fock exchange. All DFAs have difficulties describing the energy of the water molecule in reactions $R_4$. If we exclude that reaction from the average, with 10% HF, the resulting standard enthalpies of formation of 424 ± 2 and 183 ± 3 kJ $mol^{-1}$ for RuO and $RuO_2$ are those that are closest to the CCSD(T) values, though the deviations are of 7 and 32 kJ $mol^{-1}$, respectively.

**Calculation of Standard Molar Entropy of Formation and Heat Capacity Constants.** From the molecular properties obtained at the TPSSh-5%HF/aug-cc-pVTZ level, the standard molar entropies [$S^\circ$(298 K)] and heat capacities at constant pressure $C_p$ (298 K) are presented in Table 11. The fit coefficients of the heat capacity function $C_p(T) = a + bT + cT^2 + dT^{-2}$ are presented in Table S4 and displayed in Figures S1−S3 of the Supporting Information.

**Table 11. Calculated Standard Molar Entropies at 298 K [$S^\circ$(298 K)] and Heat Capacities [$C_p$(298 K)] in J $K^{-1}$ $mol^{-1}$ for the Gaseous Ruthenium Oxides Computed at the TPSSh-5%HF/aug-cc-pVTZ Level of Theory with Unscaled Vibrational Frequencies**

| species | Ru | RuO | $RuO_2$ | $RuO_3$ | $RuO_4$ |
|---|---|---|---|---|---|
| | $\sigma$[a] = 1 | $\sigma$ = 1 | $\sigma$ = 2 | $\sigma$ = 2 | $\sigma$ = 2 |
| $S^\circ$(298 K) | 186.6 | 242.3 | 266.4 | 291.0 | 287.5 |
| $C_p$ (298 K) | 21.52 | 31.22 | 44.46 | 60.79 | 73.51 |

[a]Symmetry number.

For Ru, the computed standard molar entropy and heat capacity are in excellent agreement with the values of the literature.[15] To compute the temperature evolution of the heat capacity, we took into account the degeneracy of Ru ground state, resulting in a different temperature profile at temperatures greater than 800 K from the Barin et al.[15] tabulated function. For both RuO and $RuO_2$, the computed standard molar entropies at room temperature and heat capacities temperature



DOI: 10.1021/acs.jpca.5b01645
J. Phys. Chem. A 2015, 119, 4961−4971

dependencies (See Table 11 and Table S4 and Figures S1 and S2 of the Supporting Information) for RuO. $RuO_2$ curves are in excellent agreement with the values used in the literature.[13,15]

For $RuO_3$ and $RuO_4$, the computed quantities exhibit slightly larger difference with the experimental values,[15] resulting in heat capacity temperature evolution curves (See Figures S2 and S3 of the Supporting Information) that differ at temperatures either lower than 1000 K and higher than 1500 K. The largest differences with the literature values (see Table 2) are sizable for the standard molar entropy of $RuO_3$, for which we predict a value of 291 J $K^{-1}$ $mol^{-1}$, while Barin et al.[15] use 276 J $K^{-1}$ $mol^{-1}$. Note that our DFT value lies within the boundaries of the value derived by Garisto,[14] 291.4 ± 3.0 J $K^{-1}$ $mol^{-1}$.

## CONCLUSION

In this paper, we have established a methodology to investigate the electronic structure and thermodynamic parameters of ruthenium compounds. This methodology has been validated using ruthenium oxides for which we have experimental data for thermodynamic quantities. Using geometries obtained at the DFT level (U-TPSSh-5%HF), we have investigated the ability of several post-HF (CCSD(T), CASSCF, MRCI, and CASPT2) approaches to provide the best improvement of the electronic correlation energies and the spin−orbit coupling. For spin−orbit treatment, apparently it is not worth going being SO-CASSCF level. The dynamic electronic correlation contributions seems to be important, so that multireference MRCI or CASPT2 approaches are not accurate enough, as compared to CCSD(T). The ground state of Ru is $^5$F, RuO $^5\Delta$, and $RuO_2$ has singlet multiplicity like $RuO_3$ and $RuO_4$. Our calculations predict the standard enthalpies of formation to be 639, 420, 140, and −50 kJ $mol^{-1}$ for Ru, RuO, $RuO_2$, and $RuO_3$, respectively.

## ASSOCIATED CONTENT

### Supporting Information

Binding energies of the ruthenium oxides, standard enthalpies of formation of the H, $H_2$, $H_2O$, OH, O, $O_2$, spin−orbit contributions to the ruthenium oxides ground-state electronic energies, entropies, and heat capacities of the ruthenium oxides. Temperature dependence of the heat capacity at constant pressure for Ru, RuO, $RuO_2$, $RuO_3$, and $RuO_4$. The Supporting Information is available free of charge on the ACS Publications website at DOI: 10.1021/acs.jpca.5b01645.

## AUTHOR INFORMATION

### Corresponding Author

*E-mail: valerie.vallet@univ-lille1.fr. Tel: +33 3 2033 5985 and +33 3 2033 7020.

### Notes

The authors declare no competing financial interest.

## ACKNOWLEDGMENTS

Computer time for part of the theoretical calculations was kindly provided by the Centre de Ressources Informatiques de Haute Normandie (CRIHAN), the Centre de Ressources Informatiques (CRI) of the University of Lille1, and the HPC Ressources from GINCI-CINES (Grant 2014-project X2014086731). The CaPPA project (Chemical and Physical Properties of the Atmosphere) is funded by the French National Research Agency (ANR) through the PIA (Programme d'Investissement d'Avenir) under contract "ANR-11-LABX-0005-01" and by the Regional Council "Nord-Pas de Calais" and the "European Funds for Regional Economic Development" (FEDER). We are very grateful to Dr. Florent Réal, Dr. André Severo Pereira Gomes, and Dr. François Virot for their constructive comments on this work. We are also thankful to Dr. Kirk Peterson for discussions on the applicability of coupled-cluster methods to transition metal molecules.

## REFERENCES

(1) Mun, C.; Cantrel, L.; Madic, C. Review of Literature on Ruthenium Behavior in Nuclear Power Plant Severe Accidents. *Nucl. Technol.* **2006**, *156*, 332−346.
(2) Mun, C.; Cantrel, L.; Madic, C. Study of $RuO_4$ Decomposition in Dry and Moist Air. *Radiochim. Acta* **2007**, *95*, 643−656.
(3) Mun, C.; Cantrel, L.; Madic, C. Radiolytic Oxidation of Ruthenium Oxide Deposits. *Nucl. Technol.* **2008**, *164*, 245−254.
(4) Auvinen, A.; Brillant, G.; Davidovich, N.; Dickson, R.; Ducros, G.; Dutheillet, Y.; Giordano, P.; Kunstar, M.; Kärkelä, T.; Mladin, M.; et al. Progress on Ruthenium Release and Transport Under Air Ingress Conditions. *Nucl. Eng. Des.* **2008**, *238*, 3418−3428.
(5) Holm, J.; Glänneskog, H.; Ekberg, C. Deposition of $RuO_4$ on Various Surfaces in a Nuclear Reactor Containment. *J. Nucl. Mater.* **2009**, *392*, 55−62.
(6) Giordano, P.; Auvinen, A.; Brillant, G.; Colombani, J.; Davidovich, N.; Dickson, R.; Haste, T.; Kärkelä, T.; Lamy, J. S.; Mun, C.; et al. Recent Advances in Understanding Ruthenium Behaviour Under Air-Ingress Conditions During a PWR Severe Accident. *Prog. Nucl. Energy* **2010**, *52*, 109−119.
(7) Brillant, G.; Marchetto, C.; Plumecocq, W. Ruthenium Release from Fuel in Accident Conditions. *Radiochim. Acta* **2010**, *98*, 267−275.
(8) Vér, N.; Matus, L.; Kunstár, M.; Osán, J.; Hózer, Z.; Pintér, A. Influence of Fission Products on Ruthenium Oxidation and Transport in Air Ingress Nuclear Accidents. *J. Nucl. Mater.* **2010**, *396*, 208−217.
(9) Pontillon, Y.; Ducros, G. Behaviour of Fission Products Under Severe PWR Accident Conditions. the VERCORS Experimental Programme−Part 3: Release of Low-Volatile Fission Products and Actinides. *Nucl. Eng. Des.* **2010**, *240*, 1867−1881.
(10) Beuzet, E.; Lamy, J. S.; Perron, H.; Simoni, E.; Ducros, G. Ruthenium Release Modelling in Air and Steam Atmospheres Under Severe Accident Conditions Using the MAAP4 Code. *Nucl. Eng. Des.* **2012**, *246*, 157−162.
(11) Vér, N.; Matus, L.; Pintér, A.; Osán, J.; Hózer, Z. Effects of Different Surfaces on the Transport and Deposition of Ruthenium Oxides in High Temperature Air. *J. Nucl. Mater.* **2012**, *420*, 297−306.
(12) Kärkelä, T.; Vér, N.; Haste, T.; Davidovich, N.; Pyykönen, J.; Cantrel, L. Transport of Ruthenium in Primary Circuit Conditions During a Severe NPP Accident. *Ann. Nucl. Energy* **2014**, *74*, 173−183.
(13) Cordfunke, E. H. P.; Konings, R. J. M. Thermochemical Data for Reactor Materials and Fission Products: The ECN Database. *J. Phase Equilib.* **1993**, *14*, 457−464.
(14) Garisto, F. *Thermodynamic Behaviour of Ruthenium at High Temperatures*; Technical Report AECL-9552, **1988**.
(15) Barin, I., Knacke, O., Kubaschewski, O. *Thermochemical Properties of Inorganic Substances*; Springer-Verlag: Heidelberg, 1977.
(16) van Dorsselaere, J. P.; Seropian, C.; Chatelard, P.; Jacq, F.; Fleurot, J.; Giordano, P.; Reinke, N.; Schwinges, B.; Allelein, H. J.; Luther, W. The ASTEC Integral Code for Severe Accident Simulation. *Nucl. Technol.* **2009**, *165*, 293−307.
(17) Panish, M. B.; Reif, L. Vaporization of Ruthenium and Osmium. *J. Chem. Phys.* **1962**, *37*, 128.
(18) Carrera, N. J.; Walker, R. F.; Plante, E. R. Vapor Pressures of Ruthenium and Osmium. *J. Res. Natl. Bur. Stand., Sect. A* **1964**, *68A*, 325.
(19) Norman, J. H., Staley, H. G., Bell, W. E. In *Advances in Chemistry: Mass Spectrometry in Inorganic Chemistry*; Margrave, J. L.,


DOI: 10.1021/acs.jpca.5b01645
J. Phys. Chem. A 2015, 119, 4961−4971

Ed.; American Chemical Society: Washington, D. C., 1968; Vol. *72*, Chapter 8, pp 101−114.
(20) Paule, R. C.; Margrave, J. L. Vapor Pressures of Platinum Metals. III. Iridium and Ruthenium. *J. Phys. Chem.* **1963**, *67*, 1896−1897.
(21) Rard, J. A. Chemistry and Thermodynamics of Ruthenium and Some of Its Inorganic Compounds and Aqueous Species. *Chem. Rev.* **1985**, *85*, 1−39.
(22) Rard, J. A. Correction: Chemistry and Thermodynamics of Ruthenium and Some of Its Inorganic Compounds and Aqueous Species. *Chem. Rev.* **1986**, *86*, 731−731.
(23) Krikorian, O. H.; Carpenter, J. H.; Newbury, R. A Mass Spectrometric Study of the Enthalpy of Sublimation of Technetium. *High Temp. Sci.* **1969**, *1*, 313−330.
(24) Pedley, J. B.; Marshall, E. M. Thermochemical Data for Gaseous Monoxides. *J. Phys. Chem. Data* **1983**, *12*, 967−1031.
(25) Glushko, V. P., Gurvich, L. V., Veits, I. V., Medvedev, V. A., Khachkuruzov, G. A., Yungman, V. S., Bergman, G. A. In *Termicheskie Konstanty Veshchestv*; Glushko, V. P., Ed.; Nauka: Moscow, 1978−1982; Vol. *1*−*4*.
(26) Bell, W. E.; Tagami, M. High-Temperature Chemistry of the Ruthenium-Oxygen System. *J. Phys. Chem.* **1963**, *67*, 2432−2436.
(27) Schäfer, H.; Schneidereit, G.; Gerhardt, W. Zur Chemie Der Platinmetalle. $RuO_2$ Chemischer Transport, Eigenschaften, Thermischer Zerfall. *Z. Anorg. Allg. Chem.* **1963**, *319*, 327−336.
(28) Schäfer, H.; Tebben, A.; Gerhardt, W. zur Chemie der Platinmetalle. V Gleichgewichte Mit $Ru_{(f)5}$ $RuO_{2(f)5}$ $RuO_{3(g)}$ Und $RuO_{4(g)}$. *Z. Anorg. Allg. Chem.* **1963**, *321*, 41−55.
(29) Alcock, C. B.; Hooper, G. W. Thermodynamics of the Gaseous Oxides of the Platinum-Group Metals. *Proc. R. Soc. A* **1960**, *254*, 551−561.
(30) Penman, B. D., Hammer, R. R. *Ruthenium Dioxide-Oxygen-Ruthenium Tetroxide Equilibrium*; Report IN 1013; **1968**.
(31) Krauss, M.; Stevens, W. J. Electronic Structure of FeO and RuO. *J. Chem. Phys.* **1985**, *82*, 5584.
(32) Frisch, M. J., Trucks, G. W., Schlegel, H. B., Scuseria, G. E., Robb, M. A., Cheeseman, J. R., Scalmani, G., Barone, V., Mennucci, B., Petersson, G. A. et al. *Gaussian 09*, revision C.01; Gaussian Inc.: Wallingford CT, 2009.
(33) Peterson, K. A.; Figgen, D.; Dolg, M.; Stoll, H. Energy-Consistent Relativistic Pseudopotentials and Correlation Consistent Basis Sets for the 4*d* Elements Y-Pd. *J. Chem. Phys.* **2007**, *126*, 124104.
(34) Dunning, T. H., Jr. Gaussian Basis Sets for Use in Correlated Molecular Calculations. I. the Atoms Boron Through Neon and Hydrogen. *J. Chem. Phys.* **1989**, *90*, 1007−1023.
(35) Polo, V.; Kraka, E.; Cremer, D. Some Thoughts About the Stability and Reliability of Commonly Used Exchange-Correlation Functionals-Coverage of Dynamic and Nondynamic Correlation Effects. *Theor. Chem. Acc.* **2002**, *107*, 291−303.
(36) Polo, V.; Kraka, E.; CREMER, D. Electron Correlation and the Self-Interaction Error of Density Functional Theory. *Mol. Phys.* **2002**, *100*, 1771−1790.
(37) Polo, V. The Role of Self-Interaction Error in Density Functional Theory, Ph.D. Thesis, Göteborg University, 2002.
(38) Tao, J.; Perdew, J. P.; Staroverov, V. N.; Scuseria, G. E. Climbing the Density Functional Ladder: Nonempirical Meta-Generalized Gradient Approximation Designed for Molecules and Solids. *Phys. Rev. Lett.* **2003**, *91*, 146401.
(39) Vydrov, O. A.; Scuseria, G. E.; Perdew, J. P.; Ruzsinszky, A.; Csonka, G. I. Scaling down the Perdew-Zunger Self-Interaction Correction in Many-Electron Regions. *J. Chem. Phys.* **2006**, *124*, 094108.
(40) Werner, H.-J., Knowles, P. J., Knizia, G., Manby, F. R., Schütz, M., Celani, P., Korona, T., Lindh, R., Mitrushenkov, A., Rauhut, G. et al. *MOLPRO*, version 2012.1, a Package of Ab Initio Programs. See http://www.molpro.net, 2012.
(41) Knowles, P. J.; Hampel, C.; Werner, H.-J. Coupled Cluster Theory for High Spin, Open Shell Reference Wave Functions. *J. Chem. Phys.* **1993**, *99*, 5219−5227.
(42) Knowles, P. J.; Hampel, C.; Werner, H.-J. Erratum: "Coupled Cluster Theory for High Spin, Open Shell Reference Wave Functions. *J. Chem. Phys.* **2000**, *112*, 3106−3107.
(43) Jiang, W.; DeYonker, J. N.; Wilson, A. K. Multireference Character for 3d Transition-Metal-Containing Molecules. *J. Chem. Theory Comput.* **2012**, *8*, 460−468.
(44) Langhoff, S. R.; Davidson, E. R. Configuration Interaction Calculations on the Nitrogen Molecule. *Int. J. Quantum Chem.* **1974**, *8*, 61−72.
(45) Andersson, K.; Malmqvist, P.-Å; Roos, B. O.; Sadlej, A. J.; Wolinski, K. Second-Order Perturbation Theory with a CASSCF Reference Function. *J. Phys. Chem.* **1990**, *94*, 5483−5488.
(46) Andersson, K.; Malmqvist, P.-Å; Roos, B. O. Second-Order Perturbation Theory with a Complete Active Space Self-Consistent Field Reference Function. *J. Chem. Phys.* **1992**, *96*, 1218−1226.
(47) Ghido, G.; Roos, B. O.; Malmqvist, P.-Å A Modified Definition of the Zeroth-Order Hamiltonian in Multiconfigurational Perturbation Theory (CASPT2). *Chem. Phys. Lett.* **2004**, *396*, 142−149.
(48) Angeli, C.; Borini, S.; Cestari, M.; Cimiraglia, R. A Quasidegenerate Formulation of the Second Order N-Electron Valence State Perturbation Theory Approach. *J. Chem. Phys.* **2004**, *121*, 4043−4049.
(49) Feller, D. Application of Systematic Sequences of Wave Functions to Water Dimer. *J. Chem. Phys.* **1992**, *96*, 6104−6114.
(50) Feller, D. The Use of Systematic Sequences of Wave Functions for Estimating the Complete Basis Set, Full Configuration Interaction Limit in Water. *J. Chem. Phys.* **1993**, *98*, 7059−7071.
(51) Helgaker, T.; Klopper, W.; Koch, H.; Noga, J. Basis-Set Convergence of Correlated Calculations on Water. *J. Chem. Phys.* **1997**, *106*, 9639−9646.
(52) Keith, T. A. *AIMAll* (version 14.11.23); TK Gristmill Software: Overland Park, KS, 2014, http://aim.tkgristmill.com.
(53) Cox, J. D., Wagman, D. D., Medvedev, V. A. *CODATa Key Values for Thermodynamics*; Hemisphere: New York, 1989.
(54) Scullman, R.; Thelin, B. The Emission Spectrum of RuO between 5000 and 6000 Å. *J. Mol. Spectrosc.* **1975**, *56*, 64−75.
(55) Raziunas, V.; Macur, G.; Katz, S. Emission Spectrum and Thermodynamic Properties of Ruthenium Monoxide. *J. Chem. Phys.* **1965**, *43*, 1010−1015.
(56) Li, R.; Peverati, R.; Isegawa, M.; Truhlar, D. G. Assessment and Validation of Density Functional Approximations for Iron Carbide and Iron Carbide Cation. *J. Phys. Chem. A* **2013**, *117*, 169−173.
(57) Moore, C. E. Atomic Energy Levels as Derived from the Analyses of Optical Spectra. *Natl. Stand. Ref. Data Ser.* **1971**, *35*, 245.
(58) Zhou, M.; Citra, A.; Liang, B.; Andrews, L. Infrared Spectra and Density Functional Calculations of $MO_2$, $MO_3$, $(O_2)MO_2$, $MO_4$, $MO_2^-$ (M = Re, Ru, Os) and $ReO_3^-$, $ReO_4^-$ in Solid Neon and Argon. *J. Phys. Chem. A* **2000**, *104*, 3457−3465.
(59) Hameka, H. F.; Jensen, J. O.; Kay, J. G.; Rosenthal, C. M.; Zimmerman, G. L. Theoretical Prediction of Geometries and Vibrational Infrared Spectra of Ruthenium Oxide Molecules. *J. Mol. Spectrosc.* **1991**, *150*, 218−221.
(60) Siegbahn, P. E. M. Binding in Second-Row Transition Metal Dioxides, Trioxides, Tetraoxides, Peroxides, and Superoxides. *J. Phys. Chem.* **1993**, *97*, 9096−9102.
(61) Kay, J. G.; Green, D. W.; Duca, K.; Zimmerman, G. L. Identification and Structures of Matrix-Isolated Ruthenium Oxide Molecules from Infrared Spectra. *J. Mol. Spectrosc.* **1989**, *138*, 49.
(62) Bader, R. F. W. A. Quantum Theory of Molecular Structure and Its Application. *Chem. Rev.* **1991**, *91*, 893−928.
(63) Bader, R. F. W. *Atoms in Molecules: A Quantum Theory*; Oxford University Press: Oxford, 1994.
(64) Matta, C. F., Boyd, R. J. In *The Quantum Theory of Atoms in Molecules*; Matta, C. F., Boyd, R. J., Eds.; Wiley-VCH: Weinheim, 2007 Chapter 1, pp 1−34.
(65) Cremer, D.; Kraka, E. Chemical Bonds Without Bonding Electron Density: Does the Difference Electron-Density Analysis Suffice for a Description of the Chemical Bond? *Angew. Chem., Int. Ed. Engl.* **1984**, *23*, 627−628.


DOI: 10.1021/acs.jpca.5b01645
*J. Phys. Chem. A* 2015, 119, 4961−4971

(66) Clark, A. E.; Sonnenberg, J.; Hay, P. J.; Martin, R. L. Density and Wave Function Analysis of Actinide Complexes: What Can Fuzzy Atom, Atoms-In-Molecules, Mulliken, Löwdin, and Natural Population Analysis Tell Us? *J. Chem. Phys.* **2004**, *121*, 2563−2570.
(67) Vallet, V.; Wahlgren, U.; Grenthe, I. Probing the Nature of Chemical Bonding in Uranyl(VI) Complexes with Quantum Chemical Methods. *J. Phys. Chem. A* **2012**, *116*, 12373−12380.
(68) Zimmerman, G. L.; Riviello, S. J.; Glauser, T. A.; Kay, J. G. Photochemical Decomposition of Ruthenium Tetroxide. *J. Phys. Chem.* **1990**, *94*, 2399−2404.
(69) Green, D. W.; Kay, J. G.; Zimmerman, G. L.; Balko, B. A. Infrared Spectrum of Ruthenium Tetroxide Isotopomers in an Argon Matrix. *J. Mol. Spectrosc.* **1989**, *138*, 62−68.



DOI: 10.1021/acs.jpca.5b01645
*J. Phys. Chem. A* 2015, 119, 4961−4971